# Development of a Test for Determining Fracture Toughness of Brazed Joints in Ceramic Materials

*Modified double cantilever beam specimen is used to measure toughness in brazed joints*

BY A. J. MOORHEAD AND P. F. BECHER

ABSTRACT. The characterization and analysis of the adherence in joints between ceramics or a ceramic and a metal are important factors in both the design and reliability of components for structural uses. However, because the failure stress of brittle systems is a function of both the flaw size and the true adherence, a strength test by itself cannot sufficiently describe the quality of a ceramic joint. On the other hand, fracture mechanics can be used to determine adherence in a fashion similar to that used to describe the bulk fracture behavior in brittle materials. We have developed a test, based on a modified applied moment, double cantilever beam specimen, that has been successfully used to measure the fracture toughness of joints between ceramics and ceramics and metals. Toughness measurements on samples of ceramics directly brazed with some of our experimental brazing filler metals showed that the brazed interfaces were at least as tough as the ceramics alone. Although the specimen and techniques have so far been used only for direct brazes (no surface pretreatment of the ceramic), we suggest that they would also be valid for joints involving thermal spraying of the ceramics prior to brazing.

## Introduction

Although monolithic ceramic materials have been widely used in the past in nonstructural applications, such as electrical insulators, crucibles, microwave windows, and pump and valve components for the chemical industry, it has been only in recent times that major efforts have been made to use ceramics in structural applications under severe operating conditions. The major impetus for most of this interest over the past decade is economics — as fuel costs have increased, so has the need for increased efficiency in a multitude of energy conversion processes.

For example, preheating of the combustion air is a proven way of markedly reducing fuel consumption in a high-temperature furnace. Various fixed-boundary heat exchangers have been used industrially for this purpose. Fuel consumption in a given process can be reduced 40% or more by using recuperation or regeneration to heat air for the burners (compared with use of ambient-temperature air for fuel combustion) with furnace gases in the range of 1300°C (2372°F) and air preheat temperatures above 800°C (1472°F). Recuperators offer significant engineering advantages over refractory regenerators in many industrial processes because they can be interfaced with small to medium size furnaces (they are smaller than refractory regenerators) and their valve and hot ducting requirements are simpler. Metallic alloys have been used predominantly for recuperator construction, but present materials such as austenitic or ferritic stainless steels cannot be used above about 850°C (1562°F). The mechanical and corrosion property limitations of metal alloys severely limit the use of metal recuperators to preheat air above about 600°C (1112°F) (Ref. 1). However, structural ceramics having good thermal conductivity, such as silicon carbide, offer considerable promise for use in high-temperature recuperators for recovering waste heat from hot flue gases at temperatures of 1200°C (2192°F) or higher.

Ceramic materials also show considerable promise for use in advanced gas turbine engines. Efficiency in a turbine engine is directly related to the maximum allowable operating temperature of the materials used in the hot section of the engine. The impetus to increase engine efficiency and performance has led to continuing improvements in material use temperatures. For example, in modern turbine engines, high-temperature superalloys can be used at temperatures up to approximately 1100°C (2012°F) without cooling (Ref. 2). However, turbine engines with ceramic components are being developed with turbine inlet temperatures of 1370°C (2498°F) (Ref. 3). Ceramic materials also offer other advantages in turbine engines, such as higher thrust-to-weight ratios, reduced coolant-air requirements, and a potentially lower cost.

A number of automotive manufacturers are also working to develop a more efficient diesel engine for cars or trucks that is able to eliminate the need for power-robbing cooling requirements, by using structural ceramics in the combustion chamber — cylinder, piston cap and valve plate. In the second generation of the uncooled-diesel engine (sometimes called adiabatic), the use of petroleum materials would be reduced even further by eliminating the oil lubricant through the use of high temperature ceramic bearings.

It is becoming more widely recognized that one of the key technologies that will enhance or restrict the use of ceramic materials in high performance applications, e.g., advanced heat engines or heat exchangers, is the ability to reliably join simple-shape components to form complex assemblies or to join unit lengths of material to form large systems. Although by careful selection of the location or through judicious design a joint in such

*Paper presented at the 14th International AWS Brazing and Soldering Conference, held April 26–28, 1983, in Philadelphia, Pa. Research sponsored by the U. S. Department of Energy under contract DE-AC05-840R21400 with Martin Marietta Energy Systems, Inc.*

*A. J. MOORHEAD and P. F. BECHER are with the Metals and Ceramics Division, Oak Ridge National Laboratory, Oak Ridge, Tenn.*

applications may not be required to withstand the full intensity of the various service conditions (such as temperature or stress) as the bulk ceramic material itself, it is of course highly desirable that a ceramic-to-ceramic or ceramic-to-metal joint be capable of operation at near-peak conditions. Although ceramic joining technology has been highly developed over the past fifty years or so, most of the effort has been expended in developing materials and techniques for applications that will see service at "low" temperatures and with low structural requirements. The development of technology for joining ceramics for use at elevated temperatures, at high stress levels, and in dirty environments has been very limited.

As part of a program to develop brazing filler metals for such advanced applications, we are studying the mechanical properties of the bonds between experimental brazing filler metals and typical structural ceramics; and one aspect of this work—the development of a test to measure the fracture toughness of brazed joints containing ceramic materials—is reported in this paper.

## Fracture Mechanics Approach to Adherence in Ceramic Joining

The characterization and analysis of the adherence between dissimilar materials are important factors, from the standpoint of both design and reliability, in such technologies as printed microelectronic circuitry, ceramic-to-metal seals, protective coatings (*e.g.,* ceramic coatings for metal turbines) and non-mechanical joining of components. Adherence is often determined via the stress (or load) required to cause separation. Strength data are useful in both (1) ascertaining a relative ranking of the adherence between systems, and (2) establishing and maintaining quality control during production. However, because the failure stress of brittle systems is a function of both the flaw size (*e.g.,* an unbonded interfacial area or void) and the adherence, a strength test by itself cannot determine the true adherence of a system. Strength test results also do not allow one to relate adherence to material variables in the region of failure—be it at the interface or in the bulk materials on either side of the interface. However, postfailure analysis can be used to augment strength data and to tell whether or not failure occurs at the interface, and the analysis may possibly reveal the defect that caused failure.

This basically raises the issue of how does one select materials to form a joint or interface to achieve the maximum adherence. One approach is to improve the chemical bonding between dissimilar materials, *i.e.,* the material(s) being joined and the adhesive media. Consideration may also be given to minimizing thermal stresses due to thermal expansion mismatch between dissimilar materials. However, the question remains, how does one determine the effect of such approaches on adherence? Measurement of the tensile, flexural or peel strengths of various interfaces are not sufficient by themselves, primarily because they are so strongly dependent on defect or flaw size. Adherence values (strengths) obtained by such tests cannot be related to the similar strengths (which are also flaw size dependent) obtained for the materials on either side of the interface.

On the other hand, fracture mechanics can be used to determine adherence in a fashion similar to that used to describe the bulk fracture behavior in brittle materials. The stress intensity factor (K) or strain energy release rate (G) can be used to determine the ease of crack propagation, either along an interface (adhesive failure) or in an adjacent phase (cohesive failure). Adherence is thus described in terms of the ability of the total system to resist fracture, which serves not only as a tool to examine adherence mechanisms, but also as an important design aid. In addition, the critical adherence fracture energies ($\gamma_{Ic}^{A}$) or the critical adherence fracture toughness values ($K_{Ic}^{A}$) obtained can be related to the values of the bulk materials comprising a joint, as well as the stress state at the interface.

The application of fracture mechanics to adherence problems to date has centered on the areas of structural adhesives and composites (Refs. 4, 5). In such applications, not only the analysis, but also the measurements of crack tip stress intensity (K), can become quite complex even for crack motion along a flat interface between two materials. The reason for this difficulty is that the stresses acting on a crack are not necessarily symmetric and combined loading modes exist (*e.g.,* Mode I: tensile, plus Mode II: shear). However, when the elastic properties E (Young's modulus) and $\mu$ (Poisson's ratio) of the two materials are comparable, in theory they must be identical (Ref. 6); but in practice, they need only approach each other (Ref. 7), and then the solution is the same as for the crack in a single phase body. This is the case for the analysis of adherence of many ceramic-to-ceramic and ceramic-to-metal brazements. The result is that one can describe adherence in terms of $K_I$, and not combined $K_I$-$K_{II}$, and a much simpler description of crack propagation is obtained.

Experimentally, determination of the adherence of a joint system is simplified by the use of the energy balance concept, equating the change in the system's strain energy (the strain energy release rate—$G_I$) with the total energy for crack propagation ($2\gamma_I$). Because the system can be defined, $G_I$ is related to $K_I$, *i.e.,*

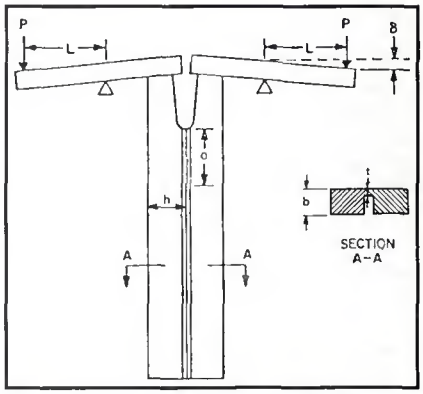


*Fig. 1—Applied moment, double cantilever beam specimen. The loading arms are typically attached by epoxy, making this essentially a room temperature test*

$$K_I = \frac{\sigma\, c^{1/2}}{A} = (G_I E)^{1/2} \qquad (1)$$

where $\sigma$ is the applied tensile stress, c is the flaw size and A is a geometric factor. Thus, either $G_I$ or $K_I$ can be determined experimentally. Several techniques have been developed to determine the adherence of not only adhesives to metal (Refs. 4, 5) but also most recently of ceramics to metals or ceramics to ceramics (Refs. 8-10).

Our approach is based on a modification of the applied moment, double cantilever beam (DCB) specimen, shown schematically in Fig. 1, which is used to determine either $K_{Ic}$ or $\gamma_{Ic}$ for bulk ceramics and glasses (Ref. 11). The modification accounts for differences in geometry or properties of the materials on either side of the interface, and is applicable as long as the thickness of any material placed at the interface, or any reaction product, is small (as is normally encountered in thick films or braze joints) (Refs. 12 and 13). Basically, the approach equates the total strain energy release rate with the interfacial energy change in each half of the double cantilever beam caused by the creation of new surfaces as the crack propagates, *i.e.,* $G_{Ic} = 2\gamma_{Ic}$. (Note that the two halves can thus be different materials or geometries.) In this case,

$$G_{Ic} = M^2 \frac{1}{EIt} = \frac{M^2}{2} \frac{1}{(EIt)_1} + \frac{1}{(EIt)_2} \qquad (2)$$

where the (M/EIt) terms determine the applied strain energy that is released in each arm during crack propagation. Referring to Fig. 1, M (= ½P·L) is the bending moment supplied by the applied load (P) acting through a fulcrum length (L) on each half of the DCB specimen, E is the Young's modulus of either half of the

DCB specimen, I is the moment of inertia, and t is the thickness of the DCB specimen in the region where the crack propagates. For the purposes of guiding the crack along the region of the interface, the specimen can be reduced in thickness by introducing a groove in that location. The moment of inertia I is based on the cross-sectional dimensions and the bending axis for each half, so that I is $bh^3/12$, where b is the thickness and h the width of each half of the DCB specimen.

The fracture toughness of both similar and dissimilar material brazements can be determined using a specimen of this type. For the similar material brazement (material in Beam 1 is the same as that in Beam 2), $K_I$ can be determined from Equation 1 with

$$G_I = G_1 + G_2 = 2G_1 \qquad (3)$$

since the materials are the same, and

$$G_1 = \tfrac{1}{2}\,\frac{\left(\frac{P}{2}\cdot L\right)^2}{E\,t\,\frac{(bh^3)}{12}} \qquad (4)$$

For the dissimilar material brazement (material in Beam 1 is not the same as in Beam 2), we want $G_1$ to be equal to $G_2$, so that the crack will not be deflected towards the beam with the higher strain energy release rate. We fix M and t so that

$$\frac{M_1^2}{t_1} = \frac{M_2^2}{t_2} \qquad (5)$$

and then by requiring that $G_1 = G_2$, it can be shown that

$$b_1h_1^3E_1 = b_2h_2^3E_2 \qquad (6)$$

Thus, by knowing the value of E in each beam, one can alter the beam dimensions to obtain $G_1 = G_2$. This solution is valid when the braze layer is thin so that the strain energy supplied to drive the crack is supplied by Beams 1 and 2.

Using this experimental approach and analysis, one can determine whether interfacial adherence failure or cohesive failure of the bulk material on either side is the limiting factor in the mechanical behavior of the joint. For the latter case, the $K_{Ic}$ value obtained will approach that of the bulk material in a similar material joint and that of the less tough material in the case of a dissimilar material joint. Furthermore, when adherence failure occurs at the interface, one can determine how changes in chemical or mechanical bonding or stress state at the interface improve the joint systems.

For example, in thick film conductors it was shown that for an optimally processed thick film, adherence was limited by the fracture toughness of the glass layer used in these systems to bond the metal conductor to the alumina substrate (Ref. 13). Note that this finding is consistent with the fact that the glass has the lowest fracture toughness of the materials in this system. Processing at higher temperatures degraded the adherence by changing the morphology of the glass/metal interface. Similar effects were noted in $Si_3N_4$ braze joints (Ref. 12). As shown by earlier results, this approach can also be used when ceramic/metal joints are employed.

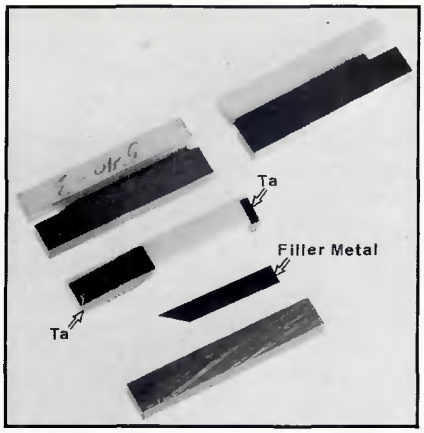


*Fig. 2 — Ceramic and metal bar as prepared for brazing and after brazing, grooving and notching (upper specimens). The wide tantalum shim and the brazing filler metal are tapered as an aid in precracking the specimen*

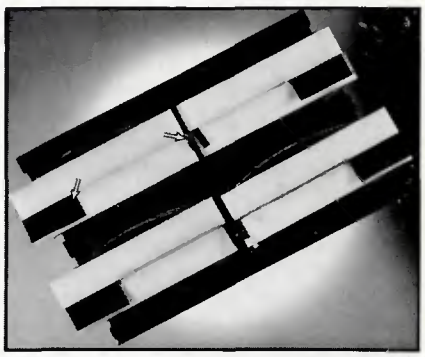

*Fig. 3 — Four composite DCB specimens in SiC boat after brazing cycle. The 0.038-mm Ta shims (arrows) are used to control braze joint thickness. The wide shims also serve as notches during specimen precracking*

#### Specimen Geometry

The overall dimensions of the typical DCB specimen used to determine the fracture toughness of a bulk ceramic are 2.5 × 9.5 × 28.5 mm (0.10 × 0.37 × 1.12 in.). A composite (brazed) specimen of similar materials is made by brazing together two beams, each having approximate dimensions of 2.5 × 4.76 × 28.5 mm (0.10 × 0.19 × 1.12 in.).

For the case of a dissimilar material specimen, the thickness (b) is held constant and the width of the beam of the material having lower modulus of elasticity is increased so that the strain energy release rate in each beam will be the same, *i.e.*, $G_1 = G_2$. If this dimension is not adjusted, during the testing the propagating crack will be deflected towards the beam with higher strain energy release rate.

For example, if a composite specimen were to contain nodular cast iron and partially stabilized zirconia (PSZ) beams (these materials being of interest for an uncooled diesel engine), Equation 6 is solved as follows for $h_{PSZ}$ = 4.76 mm:

$$\frac{E_{iron}}{E_{PSZ}} = \frac{160\ \text{GPa}}{200\ \text{GPa}} = \frac{h^3_{\ PSZ}}{h^3_{\ iron}}, \text{ or}$$

$$h_{iron} = \frac{h_{PSZ}}{0.928} = \frac{4.76\ \text{mm}}{0.928} = 5.13\ \text{mm}$$

so that the cast iron portion of the specimen would be 5.13 mm (0.20 in.) wide. For a specimen containing aluminum oxide brazed to the cast iron,

$$\frac{E_{iron}}{E_{alumina}} = \frac{160\ \text{GPa}}{350\ \text{GPa}} = \frac{h^3_{\ alumina}}{h^3_{\ iron}}$$

$$\text{or } h_{iron} = \frac{h_{alumina}}{0.771}$$

so that for a "standard" specimen (an alumina beam width of 4.76 mm/0.19 in.) the width of the cast iron beam is 6.17 mm (0.24 in.).

## Experimental Procedure

The assembly and brazing of the composite DCB specimen is not difficult if a reasonable amount of care is taken. The ceramic (or ceramic and metal) beams are placed in a ceramic fixture with a piece of brazing filler metal foil at the interface. Although some specimens were made using filler metals in the form of small pieces cut from an arc melted ingot, in many cases complete flow through the joint was not achieved; therefore, the preference was to preplace foil in the joint. The filler metal foils were made either by melt spinning, a process capable of producing a thin strip even from alloys having low ductility, or by cold rolling. In order to hold the filler metal in place during assembly, a tiny drop of cement was applied to one end. Experimentation with both fine wires and thin foils between the specimen halves to control the final thickness of the braze joint (a critical variable in any brazement) resulted in a preference for 0.038-mm (0.001-in.) thick Ta sheet, since sheet is easier to apply and maintain in place than wire. Small pieces of the foil are held in place by cement. A sample with tantalum shims in place is seen in Fig. 2.

Experimentation was also conducted with various materials and designs of springs to apply a slight load across the

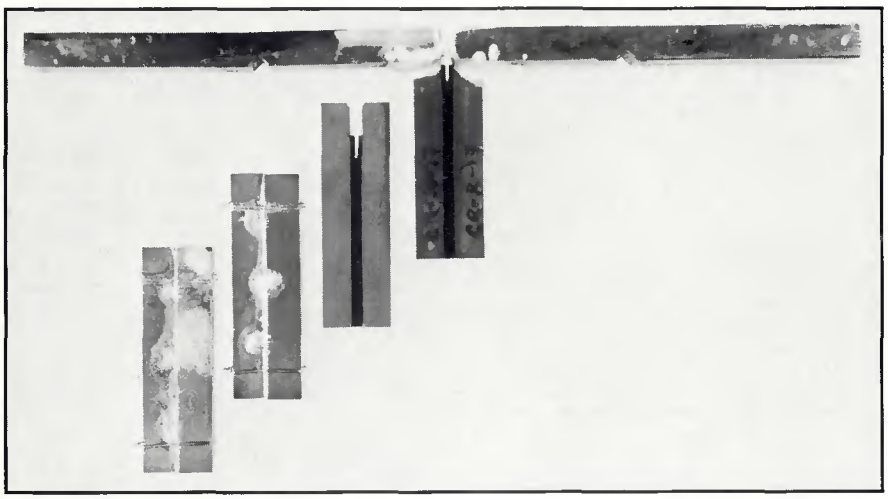

*Fig. 4 — Sequence of steps in fabrication of composite double cantilever beam specimen*

joint, and 0.25-mm (0.010-in.) thick Mo or W sheet was found to be satisfactory for the brazing temperatures used in most of the studies to date. Typical composite DCB samples in place in a SiC boat after brazing are shown in Fig. 3.

Our standard procedure for preparing the specimens is as follows: After the samples are brazed, they are ground to remove any exuded filler metal and to remove any mismatch of the surfaces. This operation is done by bonding the specimens to machining blocks using an adhesive and then machine grinding with a 170 grit diamond-abrasive wheel. After surface grinding, the specimens are grooved and notched (see fabrication sequence in Fig. 4) to insure that the crack will propagate through the region of the brazement. These operations are also done using diamond-abrasive wheels (400 grit). Next, the surface of the specimen opposite the groove is hand lapped with diamond paste (down to 3 $\mu$m). A final sharp precrack (flaw) is made in the braze joint by carefully forcing a wedge-shaped cermet tip into the large notch of the specimen. This operation is conducted under a low-power microscope so that the flaw can be observed as it forms.

As mentioned previously, the loading arms are attached using epoxy cement, taking care that the fulcrum lengths L are equal and that the specimen is perpendicular in two planes to the arms. After the epoxy is cured, the specimens are loaded in a mechanical test machine using the apparatus shown in Fig. 5. The load at failure and the specimen dimensions (b, h and t) are recorded for each test.

Catastrophic crack propagation sometimes occurs during precracking, resulting in the loss of expensive specimens. Therefore, some specimens that had not been precracked were tested, relying instead on the fine notch generated by the 0.038-mm-thick Ta shim previously described. As will be discussed below, the specimens that were not precracked gave artificially high fracture toughness numbers, so the precracking operation was reinstated for the balance of the tests.

## Materials

Some of the characteristics of the ceramic materials included in this program are given in Table 1. All of these ceramics are made by pressureless sintering except for our SiC whisker reinforced alumina composite (Ref. 14) ($Al_2O_3$-SiC), which was densified by uniaxial hot pressing in a graphite die. These specific materials were chosen because they are prime candidates for many energy conversion or utilization applications, and because they present a broad spectrum in material types and properties.

For example, SiC is the principal material being tested for high-temperature recuperator applications in waste heat environments, because of its excellent thermal conductivity and strength.

However, in some recuperator installations, such as those on aluminum remelt and glassmaking furnaces, SiC ceramics are degraded by certain halide species in aluminum melting and alkali oxides in glassmaking. In these applications, alumina or an alumina-matrix composite may prove to be a superior material.

Partially stabilized zirconia ceramics have low thermal conductivity, high toughness (for a ceramic), and relatively high thermal expansion, and are, therefore, the prime candidates for insulating the combustion chamber of the uncooled diesel engine. However, the microstructures of the PSZ's available today are not stable above about 1000°C (1832°F). They are less tough and strong at elevated temperatures (due to the reduced tendency for the tetragonal-to-monoclinic phase transformation that gives them strength and toughness). Therefore, alumina or an alumina matrix composite may emerge as a more viable candidate material. Although there is presently considerable interest in $Si_3N_4$ ceramics, this material was not included in the study. The impurity and additive levels of $Si_3N_4$ materials available today vary quite widely, making it difficult to select a representative material.

Ceramic-metal brazements have also been included in our fracture mechanics studies. A major impetus is the attachment of a ceramic piston cap to a metal piston — a joint that is critical to the success of the uncooled diesel engine (Ref.

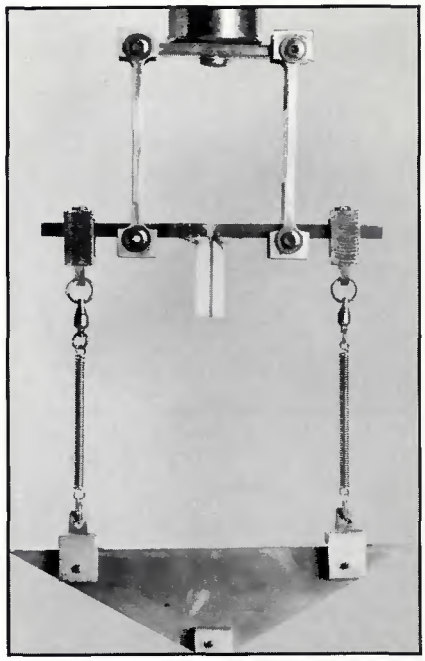

*Fig. 5 — Apparatus for testing of DCB specimens in mechanical test machine*

**Table 1—Characteristics of Ceramic Materials Brazed in This Program**

| Material Designation | Flexural Strength (MPa) | Average[a] Surface Roughness ($\mu$m) |
|---|---|---|
| Coors AD-99 alumina | 230 | 0.74 |
| Coors AD-998 alumina | 207 | 2.65 |
| Degussit AL-23 alumina | 156 | 4.46 |
| Nilsen PSZ (82-94159N) | 616 | 0.94 |
| Nilsen PSZ (83-064MS) | 574 | 0.94 |
| $Al_2O_3$-SiC[b] | 650 | |
| $\alpha$-SiC[c] | 348 | 0.70 |

[a]Determined by profilometer.
[b]SiC-whisker-reinforced alumina under development at ORNL.
[c]Hexoloy SA, Standard Oil Engineered Materials Co.

**Table 2—Fracture Toughness of Ceramic-to-Ceramic Brazed DCB Specimens**

| Ceramic Material | Brazing Filler Metal Composition (at.-%) | Brazing[a] Temperature (°C) | Number of Specimens | Fracture Toughness, $K_{Ic}$ (MPa · $m^{1/2}$) | Standard Deviation |
|---|---|---|---|---|---|
| PSZ (82-94159N)[b] | Cu-27Ag-26Ti | 1000 | 3 | 6.6 | 0.55 |
| PSZ (82-94159N) | Cu-46Ag-4Sn-1Ti | 800 | 1 | 5.2 | – |
| PSZ (85-230MS)[c] | Cu-46Ag-4Sn-1Ti | 800 | 2 | 7.4 | 0.07 |
| PSZ (82-94159N) | Cu-44Ag-4Sn-4Ti | 800 | 2 | 5.0 | 0.35 |
| PSZ (82-94159N) | Cu-44Ag-4Sn-4Ti | 825 | 2 | 4.8 | 0.85 |
| PSZ (85-230MS) | Cu-44Ag-4Sn-4Ti | 850 | 2 | 12.2 | 1.06 |
| AL-23[d] | Cu-44Ag-4Sn-4Ti | 800 | 2 | 6.3 | 0.85 |
| AL-23 | Cu-44Ag-4Sn-4Ti | 850 | 2 | 6.8 | 0.35 |
| AD-998[d] | Cu-44Ag-4Sn-4Ti | 800 | 2 | 5.4 | 1.13 |
| AD-998 | Cu-44Ag-4Sn-4Ti | 850 | 1 | 6.6 | – |

[a]All specimens brazed for 5 minutes at temperature in vacuum of <7 mPa ($5 \times 10^{-5}$ mm Hg).
[b]Fracture toughness ($K_{Ic}$) of ceramic was 6 MPa · $m^{1/2}$.
[c]$K_{Ic}$ = 14 MPa · $m^{1/2}$.
[d]$K_{Ic}$ = 4.5 MPa · $m^{1/2}$.

**Table 3—Fracture Toughness of Ceramic-Metal DCB Specimens Brazed with Experimental Filler Metals**

| Specimen Number | Materials | Filler Metal Composition (at.-%) | Brazing[a] Temperature (°C) | Fracture Toughness (MPa · $m^{1/2}$) |
|---|---|---|---|---|
| 530.4 | PSZ[b]/NCI[c] | Cu-46Ag-4Sn-1Ti | 800 | 4.6 |
| 533.1 | PSZ/Ti[d] | Cu-46Ag-4Sn-1Ti | 800 | 9.9 |
| 537.1 | PSZ/Ti | Cu-46Ag-4Sn-1Ti | 775 | 5.6 |
| 540.1 | PSZ/Ti | Cu-46Ag-4Sn-1Ti | 775 | 2.8 |
| 540.2 | PSZ/Ti | Cu-46Ag-4Sn-1Ti | 775 | 4.2 |
| 545.1 | SCW-76[e]/K-1628[f] | Cu-46Ag-4Sn-1Ti | 800 | 10.4 |
| 545.3 | SCW-76/K-162B | Cu-44Ag-4Sn-4Ti | 800 | 9.3 |

[a]All brazes in vacuum of less than 7 mPa ($5 \times 10^{-5}$ mm Hg) with hold time of 5 min at temperature.
[b]PSZ ceramic 85-230 MS.
[c]Nodular cast iron.
[d]Chemically pure titanium.
[e]SCW-76 is ceramic composite made by ORNL consisting of alumina and 20 vol-% SiC whiskers.
[f]K-1628 is a TiC cermet made by Kennametal, Inc., Raleigh, N. C.

**Table 4—Fracture Toughness of Brazed Ceramic-Ceramic DCB Specimens That Were Not Precracked Prior to Testing**

| Beam Material | Filler Metal Composition[a] (at.-%) | $K_{Ic}$ (MPa · $m^{1/2}$) | Precrack |
|---|---|---|---|
| AD-998[b] | | 4.5[c] | Yes |
| AD-998 | Cu-46Ag-4Sn-1Ti | 7.2 ± 0.3 | No |
| SiC[d] | | 4.0[c] | Yes |
| SiC | Cu-46Ag-4Sn-1Ti | 5.6 ± 1.6 | No |
| SiC | Cu-44Ag-4Sn-4Ti | 5.7 ± 0.7 | No |
| PSZ82[e] | | 6.0[c] | Yes |
| PSZ82 | Cu-27Ag-26Ti | 6.6 ± 0.6 | Yes |
| PSZ82 | Cu-44Ag-4Sn-4Ti | 4.9 ± 0.6 | Yes |
| SCW-76[f] | | 8.0[c] | Yes |
| SCW-76 | Cu-46Ag-4Sn-1Ti | 11.8 | No |

[a]All specimens brazed at 800°C for 5 min in vacuum of <0.5 mPa ($4 \times 10^{-6}$ torr).
[b]AD-998 alumina, Coors Porcelain Co.
[c]Value for toughness of bulk ceramic.
[d]Hexoloy SA, Standard Oil Engineered Materials Co.
[e]MgO stabilized.
[f]$Al_2O_3$ – 20 vol-% SiC whiskers, composite hot-pressed at ORNL.

15). The principal piston material being considered to date is nodular cast iron (NCI). This material is widely used in many conventional diesel engines (aluminum is also used). In addition to NCI, other metals (such as Ti and a TiC cermet) that might serve as transition materials to accommodate mismatches in coefficients of expansion between a ceramic cap and metal piston were experimented with.

## Experimental Results

### Fracture Toughness of Ceramic-Ceramic Brazements

The results of the room temperature tests of the composite DCB specimens of alumina and PSZ joined with some of our experimental brazing filler metals are given in Table 2. Note that the critical fracture toughness, $K_{Ic}$, of the brazed samples was generally similar to that of the bulk ceramic.

### Fracture Toughness of Ceramic-Metal Brazement

The same procedure was used for fabricating the ceramic-metal fracture toughness specimens as was previously described for the ceramic-ceramic brazed specimens. The only difference was that the width of the beam of the material having lower modulus of elasticity was increased as discussed in the section on specimen geometry. A potential problem area did arise, however, in the case of the ceramic-metal specimens, as there was a possible mismatch in coefficients of thermal expansion of the materials. The results of one such mismatch will be discussed below. When the coefficients of expansion of the ceramic and metal are relatively close, good fracture toughness values for these brazements were obtained, as shown by the data in Table 3.

### Fracture Toughness of Specimens Not Precracked

The fracture toughness data for a series of specimens that were not precracked prior to testing are given in Table 4. Note that these were all ceramic-ceramic brazements to avoid any influence on the results of residual stresses that might be generated at the interface of a ceramic-metal braze.

## Discussion of Results

Difficulty was initially experienced in fabricating the first of the ceramic-metal composite DCB specimens. Two of four NCI-to-PSZ brazements made in vacuum at 800°C (1472°F) were found to have failed by major cracking in the ceramic (Fig. 6) after the surface grinding step. The other two specimens (brazed with the same filler metal but at 825°C/1517°F) survived the surface grinding operation. However, when they were cemented to a machining block for grooving, it was observed that both the ceramic and metal portions of the specimen had been distorted by an apparent mismatch in coefficients of thermal expansion. This effect can be seen in Fig. 7. The magnitude of the deflection in the PSZ ceramic was 0.45 mm (0.017 in.),

certainly a major value for a ceramic.

The failures and distortion that occurred in the PSZ-to-NCI specimens were somewhat puzzling, as one favorable attribute of PSZ is its purported close match in coefficient of thermal expansion with that of NCI. However, when thermal expansion data were taken for this particular PSZ, the existence of a large hysteresis loop was found, as shown in Fig. 8. X-ray diffraction examination revealed that this ceramic did not contain the approximately 50% toughening tetragonal phase that is typical for other materials of this type, but, in fact, was almost fully monoclinic at room temperature. Apparently, some deviation in processing led to a ceramic that readily transforms to tetragonal on heating and back to monoclinic on cooling, and this latter transformation resulted in failure, or at least major distortion, of our brazed composite specimens.

These tests were repeated, but with a more recently manufactured sample of PSZ ceramic, identified as 85-230 MS. This ceramic contains about 25% monoclinic phase and a coefficient of thermal expansion of $10.8 \times 10^{-6}/°C$. Accordingly, the material does not have the large hysteresis loop in its thermal expansion curve. In these latest specimens, the amount of distortion in the PSZ (due to mismatch in expansion with the nodular cast iron) averaged 0.11 mm (0.004) over a length of 28 mm (1.1 in.) versus 0.45 mm (0.018 in.) for the earlier specimens. The fracture toughness data for composite DCB specimens containing this material and nodular cast iron or titanium are also given in Table 3.

Based on analysis of the data for the unprecracked specimens and low-power optical examination of the fracture surfaces, we concluded that, although the fractures did occur at the interface as

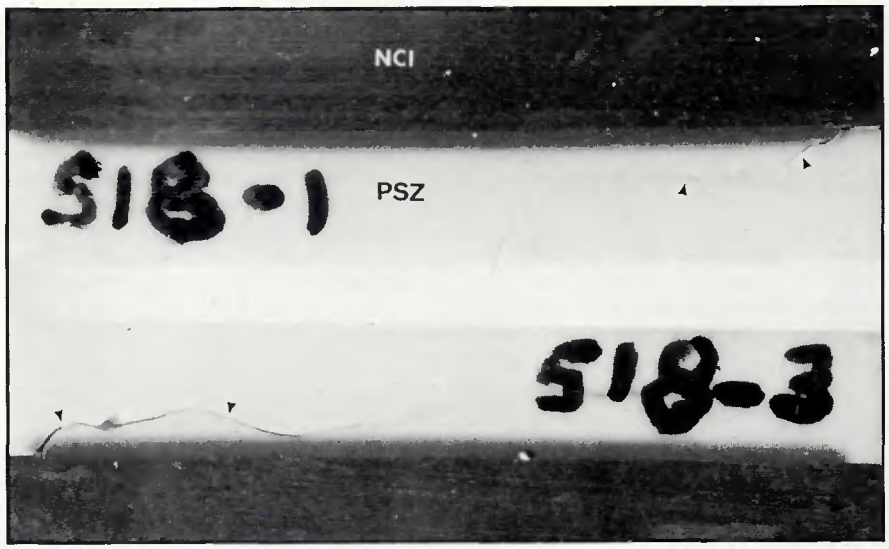


*Fig. 6 — Two ceramic-metal brazed DCB specimens showing cracking in the PSZ (arrows), apparently resulting from mismatch in coefficients of thermal expansion of the NCI and PSZ (82-94159N). The cracks have originated at the notch left by removal of gap-controlling shims*

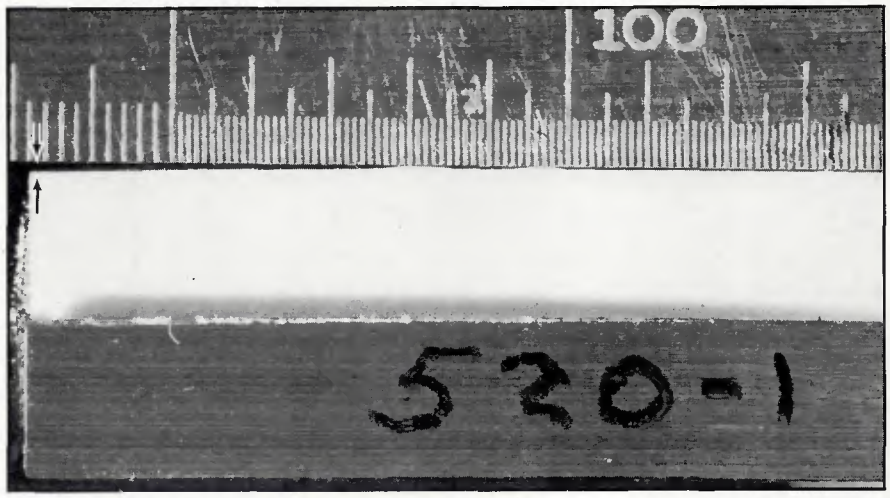


*Fig. 7 — Ceramic-metal DCB (brazed 5 min at 800°C) showing 0.45-mm (0.018-in.) distortion in the zirconia portion of the brazement. Scale markings in 100th of an inch*

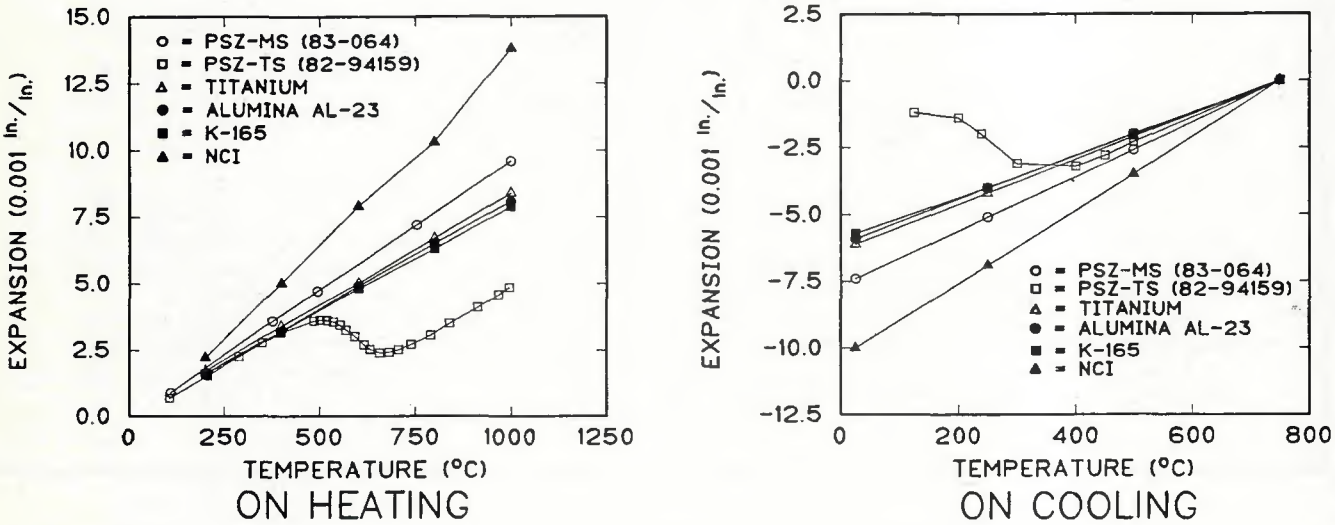


*Fig. 8 — Differences in coefficient of expansion play a crucial role in the brazing of ceramics to metals*

intended, these results are not valid. This conclusion was based on the observation that the toughness measured is in all cases higher than that of the respective bulk ceramic. With the DCB configuration, if a braze joint were significantly tougher than the bulk ceramic, the crack would quickly jump out of the interface into the adjoining ceramic. This apparently did not occur, although admittedly it is difficult to distinguish between the ceramic and nonmetallic phases that occur in the braze joint at the interface between the brazing filler metal and the ceramic. We think that the high $K_{Ic}$ values are the result of the fact that a crack "pop-in" load is always higher than the load (stress) required for propagation of a sharp flaw (precrack). Thus, when the artificially high load is used in the calculation, a higher toughness value is given.

## Conclusions

We have demonstrated that a modified applied moment, double cantilever beam specimen can be used to determine the fracture toughness of ceramic-ceramic and ceramic-metal brazements. The normal care used in preparing ceramics for all mechanical property tests must be used, but, other than that, the assembly techniques and fixture used for alignment during brazing should not pose a problem to others seeking to apply this test. We tried unsuccessfully to eliminate the most difficult aspect of the technique, precracking, but concluded that unprecracked specimens gave artificially high toughness values.

The DCB technique itself has several advantages over other fracture toughness tests developed for brittle materials. Toughness is determined from the load at failure and some dimensional data, but does not require measurement of the original precrack length. The sample requires very little material and is made up of single shapes with flat surfaces. The geometry lends itself well to the control of the braze joint thickness—a critical variable in the strength of any brazement and an important factor in sample reproducibility.

*Acknowledgments*

The authors would like to thank Hobart Keating and Mark Vance for preparing the specimens and conducting the experimental tests. We would also like to thank M. L. Santella and R. K. Williams for reviewing this work, and Fay Burns and A. R. McDonald for preparing the manuscript.

*References*

1. Tennery, V. J. 1981. *Economic Application, Design Analysis, and Material Availability for Ceramic Heat Exchangers.* ORNL/TM-7580, Oak Ridge National Laboratory, Oak Ridge, Tenn.

2. Miller, T. J., and Grimes, H. H. 1982. *Research on Ultrahigh-Temperature Materials—Monolithic Ceramics, Ceramic Matrix Composites, and Carbon/Carbon Composites.* NASA Lewis Research Center, Cleveland, Ohio.

3. Boyd, G. L., *et al.* Advanced gas turbine ceramic component development. *Proc. of 20th Automotive Tech. Dev. Contractors' Coordination Mtg.* Dearborn, Mich., Oct. 25-28, 1982, SAE P-120, April 1983.

4. Corten, H. T. *Fracture,* Vol. VII, H. Liebowitz, ed., pp. 676-769, Academic Press, New York, N. Y.

5. Mulville, D. R., and Vaishnav, R. H. 1974. *Proc. Symp. on Solid Mechanics.* AMMRC MS-74-81, Army Materials and Mechanics Research Center, Watertown, Mass.

6. Rice, J. R., and Sih, G. C. 1965. *J. Appl. Mech.,* Ser. E, 32(2):418-423.

7. Wu, E., and Thomas, R. L. 1969. Interfacial fracture phenomena. *Proc. 5th Int. Congress Rheol.,* Vol. 1, S. Onogi, ed., University Park Press, Baltimore, Md.

8. Elssner, G., and Pabst, R. 1975. Mechanical properties of ceramics. *Proc. Brit. Ceram. Soc.* 25:179-186, R. W. Davidge, ed.

9. Bascom, W. D., *et al.* 1978. Use of fracture mechanics concepts in testing of film adhesion. *Proc. ASTM Symp. on Adhesion Measurement of Thin Films, Thick Films, and Bulk Coatings.* K. L. Mittal, ed., pp. 63-81, ASTM-STP640, American Society for Testing and Materials.

10. Becher, P. F., and Halen, S. A. 1977. Ceramics for high performance applications—II. *Proc. 5th Army Materials Technology Conf.,* Newport, R.I., March 21-25, J. J. Burke, E. N. Lenoe, and R. N. Katz, eds., Brook Hill Publishing Co., Chestnut Hill, Mass.

11. Freiman, S. W., and Hench, L. L. 1972. *J. Am. Ceram. Soc.* 55:86.

12. Becher, P. F., and Halen, S. A. 1979. Solid state bonding of $Si_3N_4$. *Am. Ceram. Soc. Bull.* 58(6):582-583.

13. Becher, P. F., Newell, W. L., and Halen, S. A. 1978. Application of fracture mechanics to the adherence of thick films and ceramic braze joints. *Fracture Mechanics of Ceramics,* Vol. 3, R. C. Bradt, D. P. H. Hasselman and F. F. Lange, eds., pp. 463-471, Plenum Publishing Co., New York, N. Y.

14. Wei, G. C., and Becher, P. F. 1985. Development of SiC-whisker-reinforced ceramics. *Am. Ceram. Soc. Bull.* 64(2):298-304.

15. Woods, M. E., Mandler, W. F., Jr., and Scofield, T. L. 1985. Designing ceramic insulated components for the adiabatic engine. *Ibid,* 287-293.

WRC Bulletin 315
June 1986

**Stress Rupture Behavior of Postweld Heat Treated 2¼ Cr-1Mo Steel Weld Metal**
**By C. D. Lundin, S. C. Kelley, R. Menon and B. J. Kruse**

WRC Bulletin 315 complements Bulletin 277, issued in May 1982. Together, these bulletins address the creep properties of 2¼Cr-1Mo steel weld metal deposited with several different welding processes. They contain data obtained from the literature as well as from the many tests conducted on this program. The experimental data, in both reports, are for weld metal of several different carbon contents, postweld heat treated at either of two commonly used postweld heat treating temperatures.

Publication of this report was sponsored by the Subcommittee on Weld Metals and Welding Procedures of the Pressure Vessel Research Committee of the Welding Research Council. The price of WRC Bulletin 315 is $18.00 per copy, plus $5.00 for postage and handling. Orders should be sent with payment to the Welding Research Council, Ste. 1301, 345 E. 47th St., New York, NY 10017.